


Applicability of hiPSC-Derived Neuronal Cocultures and Rodent Primary Cortical Cultures for *In Vitro* Seizure Liability Assessment

Anke M. Tukker , Fiona M. J. Wijnolts, Aart de Groot, and Remco H. S. Westerink¹

Neurotoxicology Research Group, Toxicology Division, Institute for Risk Assessment Sciences (IRAS), Faculty of Veterinary Medicine, Utrecht University, NL-3508 TD Utrecht, The Netherlands

¹To whom correspondence should be addressed at Neurotoxicology Research Group, Toxicology Division, Institute for Risk Assessment Sciences (IRAS), Faculty of Veterinary Medicine, Utrecht University, PO Box 80.177, NL-3508 TD Utrecht, The Netherlands. E-mail: r.westerink@uu.nl.

ABSTRACT

Seizures are life-threatening adverse drug reactions which are investigated late in drug development using rodent models. Consequently, if seizures are detected, a lot of time, money and animals have been used. Thus, there is a need for *in vitro* screening models using human cells to circumvent interspecies translation. We assessed the suitability of cocultures of human-induced pluripotent stem cell (hiPSC)-derived neurons and astrocytes compared with rodent primary cortical cultures for *in vitro* seizure liability assessment using microelectrode arrays. hiPSC-derived and rodent primary cortical neuronal cocultures were exposed to 9 known (non)seizurogenic compounds (pentylentetrazole, amoxapine, enoxacin, amoxicillin, linopirdine, pilocarpine, chlorpromazine, phenytoin, and acetaminophen) to assess effects on neuronal network activity using microelectrode array recordings. All compounds affect activity in hiPSC-derived cocultures. In rodent primary cultures all compounds, except amoxicillin changed activity. Changes in activity patterns for both cell models differ for different classes of compounds. Both models had a comparable sensitivity for exposure to amoxapine (lowest observed effect concentration [LOEC] 0.03 μM), linopirdine (LOEC 1 μM), and pilocarpine (LOEC 0.3 μM). However, hiPSC-derived cultures were about 3 times more sensitive for exposure to pentylentetrazole (LOEC 30 μM) than rodent primary cortical cultures (LOEC 100 μM). Sensitivity of hiPSC-derived cultures for chlorpromazine, phenytoin, and enoxacin was 10–30 times higher (LOECs 0.1, 0.3, and 0.1 μM , respectively) than in rodent cultures (LOECs 10, 3, and 3 μM , respectively). Our data indicate that hiPSC-derived neuronal cocultures may outperform rodent primary cortical cultures with respect to detecting seizures, thereby paving the way towards animal-free seizure assessment.

Key words: alternatives to animal testing; human-induced pluripotent stem cell (hiPSC)-derived neuronal models; microelectrode array (MEA); rodent primary cortical cultures; seizure liability assessment.

Even though many test strategies are in place to detect adverse drug reactions, drug attrition still occurs frequently. Often this is due to central nervous system (CNS)-related safety issues (Arrowsmith and Miller, 2013; Onakpoya et al., 2016). A quarter of the failures occurring during clinical development is due to

CNS-related issues (Cook et al., 2014). These issues were not detected before clinical trials started, thus emphasizing the need for continued improvement of preclinical test strategies. Seizures and convulsions, defined as periods of abnormal hyper-excitability of neurons that fire in a highly synchronized

way (Easter et al., 2009; Jiruska et al., 2013), are a commonly encountered life threatening problem during preclinical drug development (Authier et al., 2016). Especially, drugs that target the CNS give a higher risk of seizures due to higher brain penetration and higher affinity for CNS targets (Gao et al., 2016). However, the potential of drugs to induce seizures is not investigated until late in the drug development process during *in vivo* studies. If seizures are detected, the need to develop alternative compounds arises, causing delays in the drug developmental process. Also, animal experiments could have been avoided if seizure liability was detected earlier in *in vitro* studies. There is thus a clear need for better CNS safety testing prior to clinical studies. Hence, it would be beneficial if a reliable high-throughput *in vitro* system becomes available for seizure liability assessment. This system would preferably use human cells to avoid interspecies translation and ethically debated animal experiments.

Currently, the acute rat hippocampal slice assay is one of the most used methods for *in vitro* seizure liability assessment (Authier et al., 2016), although brain slices have also been isolated from dogs, minipigs, and nonhuman primates (Accardi et al., 2018). Brain organization is largely maintained in this assay (Grainger et al., 2018), with active and intact neuronal networks. However, this *ex vivo* system is not suitable for high-throughput screens as slices have a short life-span (Buskila et al., 2015). Recently developed organotypic slice cultures already have a longer life-span and it has been shown that these slices can develop epileptiform activity making them a potential tool for drug screening (Magalhães et al., 2018). However, both acute and organotypic slices recordings are labor intensive and require specific expertise and equipment (Grainger et al., 2018). Also, both brain slice models are still of nonhuman origin.

Some of these drawbacks can be resolved by multiwell microelectrode array (mwMEA) recordings. This noninvasive tool makes it possible to record electrical activity of neuronal networks without affecting the integrity of the cells (for review, see Johnstone et al., 2010). All cell types that exhibit spontaneous activity can be cultured on mwMEAs, but rodent primary cortical cultures are the current gold standard (Authier et al., 2016). Primary cortical neurons grown on mwMEAs have many characteristics of *in vivo* neurons, including (spontaneous network) burst activity (Cotterill et al., 2016). The cortical cultures can be modulated with neurotransmitters and pharmacological and toxicological agents (Hogberg et al., 2011; Hondebrink et al., 2016; McConnell et al., 2012; Nicolas et al., 2014). It has been shown that rodent primary neuronal networks can be successfully used for seizure liability assessment (Bradley et al., 2018; Fan et al., 2019; Kreir et al., 2018; Tukker et al., 2020).

In vitro seizures can present themselves in different ways. According to Bradley et al. (2018), 2 patterns of *in vitro* seizurogenicity can be distinguished. Distinctive for pattern 1 is an overall increase in activity, but more important is the higher synchronicity and organization of bursts. This increased network organization is reflected in the higher number of spikes that occur within a burst (burst percentage) and the increased interspike interval coefficient of variation (ISI CoV). In the case of GABA_A receptor antagonists also an increase in burst duration can be observed. Picrotoxin (PTX), pentylenetetrazol (PTZ), and 4-aminopyridine (4-AP) are examples of compounds that match this pattern (Bradley et al., 2018). Characteristics of pattern 2 are a decrease in activity and a deterioration of organization and synchronicity reflected in a decreased ISI CoV, shorter bursts and longer interburst intervals (IBIs; Bradley et al., 2018). However, there is often only a narrow concentration window in which

this pattern is visible, because of the rapid decrease in firing rate, ultimately resulting in a silent neuronal network. Examples of compounds that match this pattern include strychnine, linopirdine, and amoxapine (Bradley et al., 2018).

The recent introduction of human-induced pluripotent stem cell (hiPSC)-derived neurons offers an interesting opportunity to circumvent the use of animals for neurotoxicity testing. These cells lack the ethical concerns of embryonic stem cells and *in vivo* experiments. hiPSC-derived neurons can be cultured on mwMEAs and develop spontaneous network activity and (network) bursting comparable with mature neurons (Odawara et al., 2016; Paavilainen et al., 2018; Sasaki et al., 2019). Also, these hiPSC-derived neuronal networks can be modulated with neurotransmitters and known neurotoxins (Tukker et al., 2016; Odawara et al., 2018). Over the last years, an increasing number of hiPSC-derived neurons became commercially available. The use of commercial iPSCs significantly reduces the time these cells need to be in culture until they develop spontaneous activity from months (Kuijlaars et al., 2016; Odawara et al., 2016) to just a few weeks (Meneghello et al., 2015; Tukker et al., 2020). This short culture duration enhances the time- and cost-efficiency of *in vitro* drug screening methods. The commercial availability also reduces the potential variability between self-cultured batches as they can be purchased in large, quality controlled quantities (Anson et al., 2011; Little et al., 2019).

For the current research, we hypothesized that hiPSC-derived neuronal cocultures are equally suitable for *in vitro* seizure liability assessment as rodent primary cortical cultures. Therefore, in this study, we investigated the potential of hiPSC-derived neuronal cocultures compared with rodent primary cortical cultures for seizure liability assessment using MEA recordings.

MATERIALS AND METHODS

Chemicals. Neurobasal-A Medium, L-glutamine, fetal bovine serum (FBS), B27 supplement (without vitamin A), N2 supplement and penicillin-streptomycin (5000 U/ml–5000 µg/ml for rat primary cortical culture media and 10 000 U/ml–10 000 µg/ml for hiPSC medium) were obtained from Life Technologies (Bleiswijk, The Netherlands). iCell Neural Supplement B and Nervous System Supplement were obtained from Cellular Dynamics International (Madison, Wisconsin). BrainPhys neuronal medium was obtained from StemCell Technologies (Cologne, Germany). Ethanol (EtOH) was obtained from VWR Chemicals (Amsterdam, The Netherlands). Laminin (L2020), 50% polyethyleneimine (PEI) solution, sodium borate, boric acid, and all other chemicals (unless described otherwise) were obtained from Sigma-Aldrich (Zwijndrecht, The Netherlands).

A set of 9 compounds was chosen as reference set (Table 1). Test concentrations were chosen based on the NC3R crack-it Neuract project and the closely related work from the HESI-MEA subteam. All reference compounds were obtained from Sigma-Aldrich. An additional set of 3 compounds (PTX, strychnine and 4-AP; Table 1) of which data were published previously (Tukker et al., 2020) has been added to the heatmaps for more extensive mode of action comparisons. Stock solutions of compounds dissolved in dimethyl sulfoxide (DMSO) were stored in the freezer till further use. Solutions of compounds dissolved in medium or EtOH were freshly prepared on the day of the experiment.

Cell cultures. Both rat primary cortical cells and hiPSC-derived neuronal cocultures were cultured at 37°C in a humidified 5%

Table 1. Compound Reference Set, Including Solvent Used and Reported Mode(s) of Action

Compound	Solvent	Description	CAS No.	Concentration Range (μM)	References
PTZ	Medium	GABA _A receptor antagonist, used in research as kindling model in mice and rats	54-95-5	30–3000	Dhir (2012) and Singh et al. (2019)
PTX ^a	EtOH	GABA _A receptor antagonist, used in research to induce seizures	124-87-8	0.1–10	Mackenzie et al. (2002)
Amoxapine	DMSO	Tricyclic antidepressant, blocks reuptake of norepinephrine and serotonin, also blocks the dopamine receptor. Reported to cause seizures	14028-44-5	0.03–10	Kapur et al. (1999) and Kumlien and Lundberg (2010)
Strychnine-HCl ^a	DMSO	Glycine receptor antagonist, known to induce seizures in humans and rats	1421-86-9	0.3–30	Alachkar et al. (2018) and Burn et al. (1989)
Enoxacin (sesquihydrate)	DMSO	Broad-spectrum antibiotic acting as GABA _A receptor antagonist. Known to trigger seizures and/or lower seizure threshold	84294-96-2	0.1–10	De Sarro et al. (1993) and Kawakami et al. (1997)
Amoxicillin	Medium	Antibiotic acting as GABA _A receptor antagonist. Reported to be epileptogenic	26787-78-0	1–100	Raposo et al. (2016)
Linopirdine-HCl	DMSO	Kv7.x channel blocker that enhances the release of neurotransmitter. Reported to cause epileptic behavior in rat hippocampal slices	105431-72-9	1–100	Maslarova et al. (2013) and Qiu et al. (2007)
4-AP ^a	Medium	Potassium channel blocker, used to induce seizures in <i>in vivo</i> experiments	504-24-5	1–100	Peña and Tapia (2000)
Pilocarpine-HCl	Medium	Muscarinic acetylcholine (ACh) receptor agonist used as eye-drop against high eye pressure. Also used as <i>in vivo</i> model for epilepsy	54-71-7	0.3–30	Marchi et al. (2007) and Zimmerman (1981)
CPZ-HCl	Medium	Antipsychotic drug, antagonist of dopamine D ₂ receptor. Reported to cause seizures	69-09-0	0.1–10	Boyd-Kimball et al. (2018) and Kumlien and Lundberg (2010)
Phenytoin	DMSO	Antiseizure medication by causing a block of voltage gated sodium channels	57-41-0	0.3–100	Rogawski and Löscher (2004)
Acetaminophen	EtOH	Cyclooxygenase 2 (COX-2) inhibitor used to treat pain and fever, included as negative control	103-90-2	100	Aminoshariae and Khan (2015)

^aData described and shown in Tukker et al. (2020).

CO₂ incubator. All cell culture surfaces were precoated with 0.1% PEI solution diluted in borate buffer (24 mM sodium borate/50 mM boric acid in Milli-Q adjusted to pH 8.4).

For each plating round, primary rat cortical cells were isolated from postnatal day (PND) 1 Wistar rat pups (Envigo, Horst, The Netherlands) in accordance with Dutch law and approved by the Ethical Committee for Animal Experimentation of Utrecht University. Cells obtained from the Wistar rat cortices were pooled, meaning that the resulting cultures consist of cells derived from male and female pups. Animals were treated humanely and all efforts were made to alleviate suffering. Cortical cultures were prepared as described previously (Dingemans et al., 2016; Tukker et al., 2016). Briefly, PND1 pups were decapitated and cortices were rapidly dissected on ice and kept in dissection medium (Neurobasal-A supplemented with 25 g/l sucrose, 450 μM L-glutamine, 30 μM glutamate, 1% penicillin/streptomycin, and 10% FBS, pH 7.4) during the entire procedure. Cortices were dissociated to a single-cell suspension by mincing, trituration and filtering through a 100 μm mesh (EASYstrainer, Greiner). The cell suspension was diluted to 2×10^6 cells/ml. Then, a 50 μl droplet was placed on the electrode field of a precoated 48-well MEA plate (Axion BioSystems Inc., Atlanta, Georgia). Cells were left for approximately 2 h to adhere before adding 450 μl dissection medium. To prevent glial overgrowth, 90% of the dissection medium was replaced by

glutamate medium (Neurobasal-A supplemented with 25 g/l sucrose, 450 μM L-glutamine, 30 μM glutamate, 1% penicillin/streptomycin, and 2% B-27 supplement, pH 7.4) at day *in vitro* (DIV) 1 resulting in a culture with \pm 46% astrocytes (Tukker et al., 2016). At DIV4, 90% of the glutamate medium was replaced with FBS medium (Neurobasal-A supplemented with 25 g/l sucrose, 450 μM L-glutamine, 1% penicillin/streptomycin, and 10% FBS, pH 7.4).

For each plating round, iCell Glutaneurons (Lot No. 103288, male donor, containing \pm 70% glutamatergic neurons, and 30% GABAergic neurons; Cellular Dynamics International) and iCell Astrocytes (Lot No. 103956 or 11493, female donors; Cellular Dynamics International) were thawed and cultured according to manufacturer's protocol as described previously (Tukker et al., 2020). Briefly, cells were thawed separately in BrainPhys medium supplemented with 2% iCell Neural Supplement B, 1% Nervous System Supplement, 1% N2, 1% penicillin-streptomycin (10 000 U/ml–10 000 $\mu\text{g}/\text{ml}$), and 0.1% laminin. The cell pellet was dissolved in dotting medium (ie, supplemented BrainPhys medium with 10% laminin). Before plating, iCell Glutaneurons and iCell Astrocytes were premixed into a coculture containing 15×10^3 iCell Glutaneurons/ μl and 6.7×10^3 iCell Astrocytes/ μl so that each well contains 120×10^3 iCell Glutaneurons and 20×10^3 iCell Astrocytes. Cells were plated in 11 μl droplets (140×10^3 cells/droplet with 85% iCell

Glutaneurons, and 15% iCell Astrocytes) over the electrode field of 48-well MEA plates. Following plating, cells were allowed to adhere for approximately 1 h after which 300 μ l of room temperature (RT) supplemented BrainPhys medium was added. Hereafter, 50% medium changes with RT supplemented BrainPhys medium took place at DIV1, 2, 4, 6, 8, 10, 12, and 14.

MEA recordings. Each well of a 48-well MEA plate contains 16 nanotextured gold microelectrodes (approximately 40–50 μ m diameter; 350 μ m spacing) with 4 integrated ground electrodes. This yields a total of 768 channels that can be recorded simultaneously (for review, see [Johnstone et al., 2010](#)). Spontaneous electrical activity was recorded as described previously ([Nicolas et al., 2014](#); [Tukker et al., 2019](#)). Briefly, signals were recorded, in the absence of extra CO₂, at the day of experiments (DIV9–11 for rat primary cortical cultures or DIV14 for hiPSC-derived cocultures) using a Maestro 768-channel amplifier with integrated heating system and temperature controller and a data acquisition interface (Axion BioSystems Inc., Atlanta, Georgia). Data acquisition was managed with Axion's Integrated Studio (AxIS 2.4.2.13) and recorded as .RAW files. All channels were sampled simultaneously with a gain of 1200 \times and a sampling frequency of 12.5 kHz/channel, using a 200–5000 Hz band-pass filter. Prior to the recording, MEA plates were allowed to equilibrate for 5–10 min in the Maestro.

In order to determine the effects of reference compounds on spontaneous neuronal activity (spiking and [network] bursting behavior) on the 2 types of cell cultures, a 30 min baseline recording was made. Following this recording, wells were exposed (10 \times dilution for primary rat cortical cultures, 30 \times dilution for hiPSC-derived cocultures) to the reference compounds or the appropriate solvent control. Test concentrations were determined by the NC3R's CRACK-it team, who based their choice on the list of the HESI NeuTox MEA Subteam. Then activity was recorded for another 30 min. Stock solutions of compounds dissolved in DMSO or EtOH were diluted in culture medium to obtain desired concentrations. In all experiments, the solvent concentration never exceeded 0.1% v/v. In order to prevent receptor (de)sensitization, each well was exposed to a single concentration. For each experimental condition, MEA plates from at least 2 different plating rounds were used.

Data analysis and statistics. To determine (modulation of) spontaneous activity, .RAW data files were re-recorded to obtain Alpha Map files for further data analysis. In this rerecording, spikes were detected using the AxIS spike detector (Adaptive threshold crossing, Ada BandFit v2) with a variable threshold spike detector set at 7 \times (primary cortical culture) or 5.5 \times (hiPSC culture; SD) of internal noise level (rms) on each electrode. This difference in spike detection threshold does not significantly affect effect size (see [Supplementary Figure 3](#)). Post/prespike duration was set to 3.6/2.4 ms. For further analysis, spike files were loaded in NeuralMetric Tool (version 2.2.4, Axion BioSystems). Only active electrodes (mean spike rate [MSR] \geq 6 spikes/min) in active wells (\geq 1 active electrode) were included in the data analysis. Mean number of active electrodes per well for hiPSC-derived neuronal cocultures was 12.6 and for rat primary rodent cultures 9.8 (see [Supplementary Figure 4](#)). The (network) bursting behavior was analyzed as it is crucial for (in vivo) transmission of information ([Izhikevich et al., 2003](#)) using the Poisson Surprise method ([Legéndy and Salcman, 1985](#)) with a minimal surprise of 10 and a minimum bursting frequency of 0.3 bursts/min. Network bursts were extracted with the adaptive threshold algorithm.

Effects of reference compounds on the spontaneous activity pattern were determined in exposure experiments where baseline activity prior to exposure was compared with activity following exposure. To prevent inclusion of exposure artifacts, windows for data analysis were corrected for the time it took to expose the whole plate. In other words, if exposure took 2 min, the first 2 min were not included in data analysis or when a window of 20–30 min postexposure was analyzed, analysis started at 20 + 2 min. Optimum effect windows were determined separately for all reference compounds. For all reference compounds the window of 20–30 min postexposure was used for analysis of effects.

A custom-made MS Excel macro was used to calculate treatment ratios (TRs) per well for the different metric parameters ([Table 2](#)) by: $(\text{parameter}_{\text{exposure}}/\text{parameter}_{\text{baseline}}) \times 100\%$. Hereafter, TRs were normalized to appropriate vehicle control. Outliers were identified well-based and defined as not within average $\pm 2 \times$ SD were removed (3.4% for hiPSC-derived neuronal data and 4.8% for rat primary cortical data). To test for biological relevant concentration-dependent effects, the variability around control values was defined. SD values as a percentage of the mean value per parameter of the control were calculated. This SD was added and subtracted from 100% to create effect threshold levels on that parameter. Response values above or below this threshold were marked as a "hit." This was done for every single parameter. Heatmaps were created in R (version 3.6.0) using the pheatmap package (by [Kolde, 2019](#), version 1.0.12). Data are presented as mean \pm SEM from the number of wells (n) indicated, derived from at least 2 independent plating rounds (ie, independent rodent culture isolations or thawing of vials for hiPSC-derived cocultures). As not all spiking wells show burst, and not all bursting wells show network burst, the number of wells (n) used for analysis of the different parameters may differ, in particular for treatments that lower or eliminate (network) burst activity (see [Supplementary Tables 1–11](#) for exact number of wells used for calculations). Lowest observed effect concentrations (LOECs) are defined as lowest "hit" concentrations at one of the activity parameters.

Principal component analysis. Principal component analysis (PCA) can be used to visualize the level of variation between different culture models following exposure to compounds with the same mode of action. Therefore, a PCA was performed to segregate MEA results of hiPSC-derived cocultures and rat primary cortical cultures following exposure to GABA_A antagonists (PTZ, PTX, amoxapine, enoxacin, and amoxicillin) and visualize a (potential) interspecies difference. The class of GABA_A antagonists was chosen, because they form the majority of compounds in this study. The PCA was conducted in R using the packages FactoMineR ([Lê et al., 2008](#)) and FactoExtra (by [Kassambara and Mundt, 2017](#); version 1.0.5). To prevent empty cells in the matrix, average values per parameter of the middle test concentration were calculated. Next, highly correlated parameters were removed from the data set. Correlation was determined based on visual inspection of the correlation matrix and the heatmap, resulting in removal of 10 parameters. The resulting 14 parameters included in the analysis are depicted in *italic* in [Table 2](#), including MSR, mean burst rate (MBR), mean network burst rate (MNBR), parameters related to (network) burst duration and percentage and synchronicity parameters. A scree plot was created to visualize the percentage of variation explained by each component and eigen-values were calculated. The loading of each parameter to a component was calculated. Parameters contributing more than the expected contribution of 7% [expected

Table 2. Description of Different Metric Parameters

	Metric Parameter	Description	Coding
Spike parameters	<i>MSR</i>	Total number of spikes divided by recording time (Hz)	S1
	<i>ISI CoV</i>	SD ISI (time between spikes) divided by the mean ISI. Measure for spike regularity: 0 indicates perfect spike distribution, >1 signals bursting	S2
Burst parameters	<i>MBR</i>	Total number of bursts divided by recording time (Hz).	B1
	<i>Burst duration</i>	Average time from the first spike in a burst till the last spike (s)	B2
	Number of spikes per burst	Average number of spikes occurring in a burst	B3
	Mean ISI within burst	Mean ISI within a burst (s)	B4
	Median ISI within burst	Median ISI within a burst (s)	B5
	Median/mean ISI within burst	Median / mean ISI within a burst. Values close to 1 indicate a symmetric distribution of spikes within a burst	B6
	<i>IBI</i>	Time between the last spike of a burst and the first spike of a subsequent burst (s)	B7
	<i>IBI CoV</i>	Standard deviation of IBI divided by the mean IBI. Measure for burst regularity	B8
Network burst parameters	<i>Burst percentage</i>	Percentage of total number of spikes occurring in a burst	B9
	<i>MNBR</i>	Total number of network bursts divided by recording time (Hz)	N1
	<i>Network burst duration</i>	Average time from the first spike till the last spike in a network burst (s)	N2
	Number of spikes per network burst	Average number of spikes occurring in a network burst	N3
	Mean ISI within network burst	Average of the mean ISIs within a network burst (s)	N4
	Median ISI within network burst	Median ISI within a network burst (s)	N5
	Median/mean ISI within network burst	Median / mean ISI within a network burst. Values close to 1 indicate a symmetric distribution of spikes within a burst	N6
	Number of electrodes participating in network burst	Average number of electrodes with spikes that participate in the network burst	N7
	Number of spikes per network burst per channel	Average number of spikes in a network burst, divided by the number of electrodes that participate in the network burst	N8
	<i>Network burst percentage</i>	Percentage of total spikes occurring in a network burst	N9
	<i>Network IBI CoV</i>	Standard deviation of network IBI divided by the mean network IBI. Measure of network burst rhythmicity: value is small when bursts occur at regular interval and increases when bursts occur more sporadic	N10
Synchronicity parameters	<i>Network normalized duration IQR</i>	Interquartile range of network bursts durations. Measure for network burst duration regularity: larger values indicate wide variation in duration	N11
	<i>Area under normalized cross-correlation</i>	Area under interelectrode cross-correlation normalized to the auto-correlations. The higher the value, the greater the synchronicity of the network	Sy1
	<i>Area under cross-correlation</i>	Area under interelectrode cross-correlation	Sy2
	<i>Full width at half height (FWHH) of normalized cross-correlation</i>	Width at half left height of the normalized cross-correlogram to half right height. Measure for network synchrony: the higher the value, the less synchronized the network is	Sy3
	<i>FWHH of cross-correlation</i>	Width at half left height of the cross-correlogram to the half right height	Sy4

Adapted from [Tukker et al. \(2020\)](#). Parameters in italic are included in the PCA.

value = (1/number of variables × 100%)] were considered important for a component. The 14D vector was projected on the plane created by the first 2 principal components that explained most of the variation to visualize the level of (potential) interspecies variation between the 2 models.

RESULTS

Baseline Activity of the 2 Models

In a previous study, we have shown that hiPSC-derived neuronal cocultures and rat primary cortical cultures both develop spontaneous activity with (network) bursting behavior, although with different activity patterns ([Tukker et al., 2020](#)). The

average MSR is 47.5 ± 1.13 Hz for hiPSC-derived neuronal cocultures, whereas the average is much lower for rat primary cortical cultures with a MSR of 10.5 ± 0.22 Hz ([Figure 1A](#)). The MBR is more comparable between the 2 models ([Figure 1B](#)). The average rate is 0.25 ± 0.007 Hz for the hiPSC-derived neuronal culture and 0.40 ± 0.073 for rat primary cortical cultures. The MNBR is 0.082 ± 0.003 Hz and 0.050 ± 0.001 Hz for hiPSC-derived neuronal cocultures and rat primary cortical cultures, respectively ([Figure 1C](#)).

Effects on Spontaneous Network Activity

To assess and compare the suitability of hiPSC-derived neuronal cocultures and rat primary cortical cultures for seizure

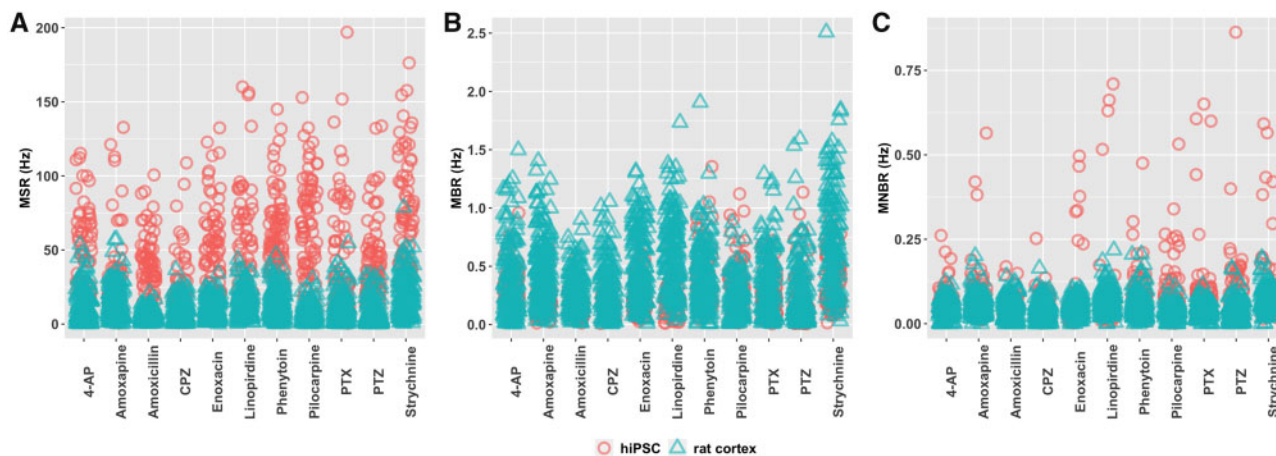


Figure 1. Characterization of baseline activity of the 2 models depicting mean spike rate (A), mean burst rate (B), and mean network burst rate (C).

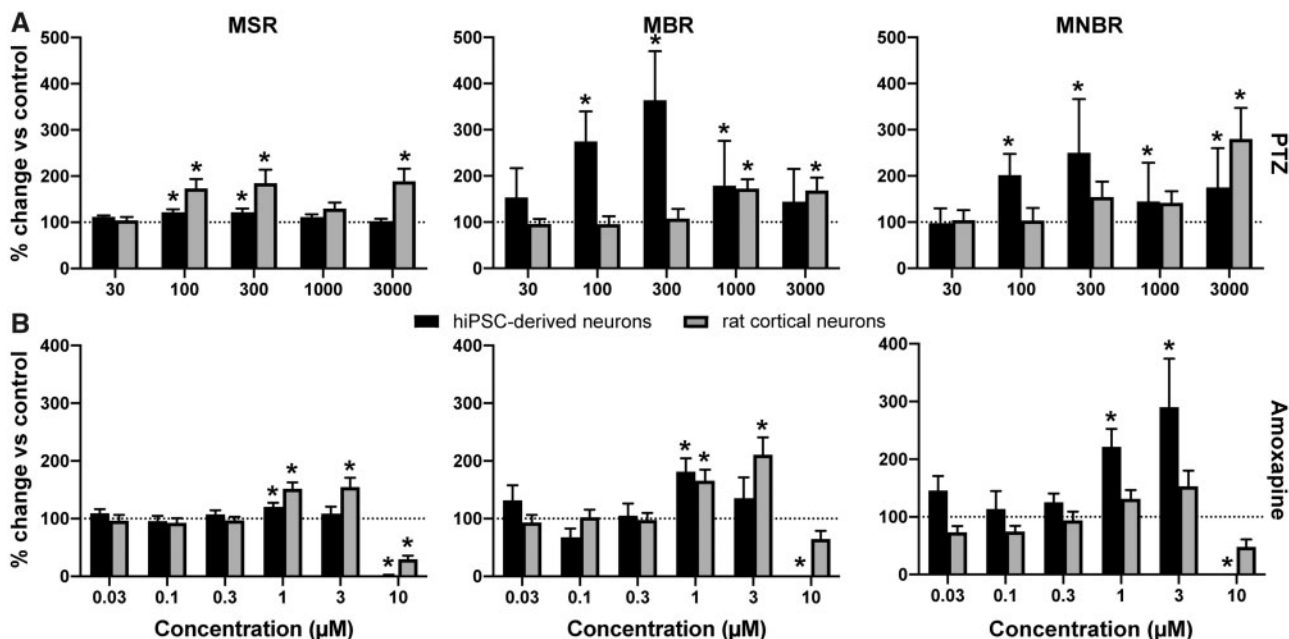


Figure 2. Effects of modulation of human-induced pluripotent stem cell (hiPSC)-derived cocultures (black) and rat primary cortical cultures (gray) with pentylene-tetrazol (A) and amoxapine (B) on mean spike rate (left), mean burst rate (middle), and mean network burst rate (right). Effects are depicted as average % change of control (solvent control set to 100%; dashed line) \pm SEM from $n = 4$ –13 wells for hiPSC-derived neuronal cocultures and $n = 13$ –33 wells for rat primary cortical cultures. * indicates a hit.

liability assessment, both models were exposed to compounds with different modes of action (Table 1). Observed neurotoxic effects were not caused by cytotoxicity (see Supplementary Figure 1).

As a negative control, cells were exposed to acetaminophen. Exposure to this compound did not result in changes in neuronal activity in rat primary cortical cultures (Zwartsen et al., 2019) or hiPSC-derived neuronal cocultures (Supplementary Figure 2).

Cys-loop receptor antagonists. In the hiPSC-derived neuronal coculture, PTZ increases MSR, MBR, and MNBR particularly at intermediate concentrations (100–300 μM ; Figure 2A). PTZ at intermediate concentration also increases the MSR in rat primary cortical cultures. At high concentrations, PTZ also increases MBR and MNBR in rat primary cortical cultures (Figure 2A).

Amoxapine increases the MSR in both cultures (1–3 μM), but at the highest concentration tested (10 μM), a strong decrease in activity occurs (Figure 2B, left). The same trend occurs in the MBR (Figure 2B, middle) and MNBR (Figure 2C, right). Overall, exposure to amoxapine increases activity in both models, but activity decreases following exposure to 10 μM .

Antibiotics. MSR of hiPSC-derived neuronal cocultures is only slightly affected following exposure to enoxacin (Figure 3A, left), although biologically relevant decreases occur following exposure to 0.3, 1, and 10 μM . Contrary, an increase can be observed when rat primary cortical cultures are exposed to enoxacin (3–10 μM). Enoxacin has little effect on MBR of hiPSC-derived cocultures, but increases MBR at the highest test concentration (10 μM) in rat primary cortical cultures (Figure 3A, middle). At low-test concentrations (0.1 and 1 μM), enoxacin

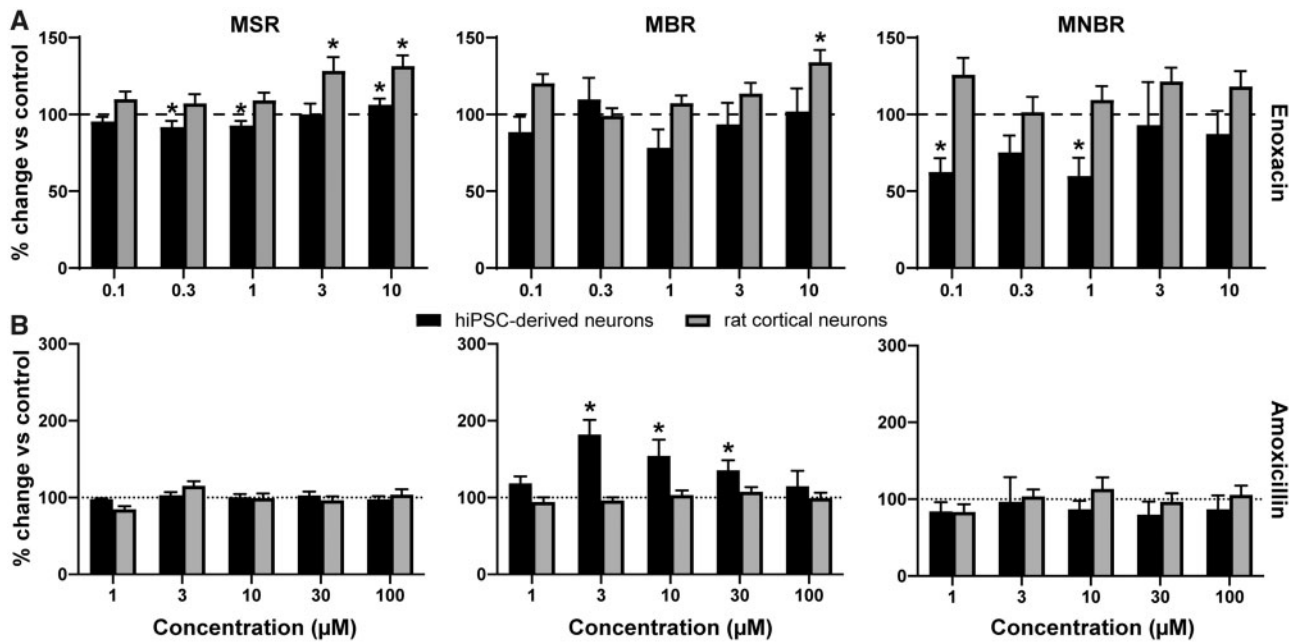


Figure 3. Effects of modulation of human-induced pluripotent stem cell (hiPSC)-derived cocultures (black) and rat primary cortical cultures (gray) with enoxacin (A) and amoxicillin (B) on mean spike rate (left), mean burst rate (middle), and mean network burst rate (right). Effects are depicted as average % change of control (solvent control set to 100%; dashed line) \pm SEM from $n = 10$ –12 wells for hiPSC-derived neuronal cocultures and $n = 26$ –35 wells for rat primary cortical cultures. * indicates a hit.

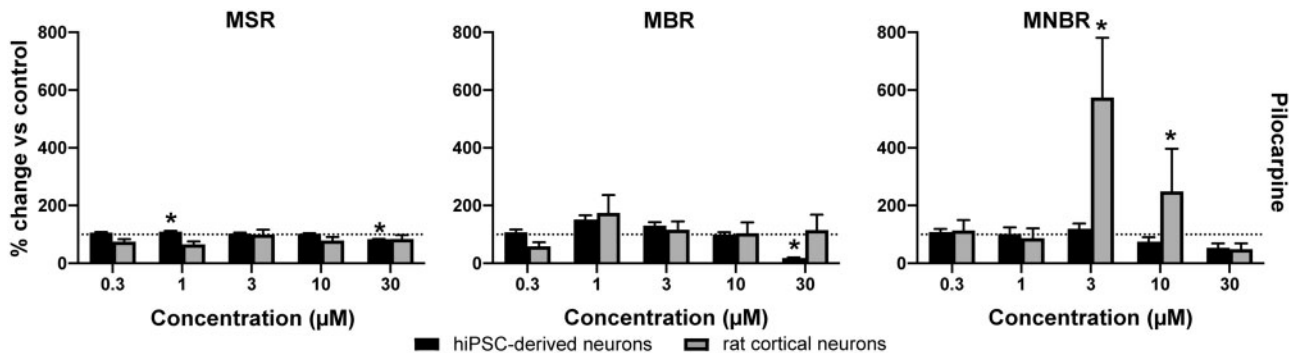


Figure 4. Effects of modulation of human-induced pluripotent stem cell (hiPSC)-derived cocultures (black) and rat primary cortical cultures (gray) with pilocarpine on mean spike rate (A), mean burst rate (B), and mean network burst rate (C). Effects are depicted as average % change of control (solvent control set to 100%; dashed line) \pm SEM from $n = 9$ –12 wells for hiPSC-derived neuronal cocultures and $n = 15$ –24 wells for rat primary cortical cultures. * indicates a hit.

decreases MNBR in hiPSC-derived cocultures, but enoxacin has little effect on MNBR in rat primary cortical cultures (Figure 3A, right).

Amoxicillin has no effect on MSR or MNBR in either of the models (Figure 3B, left/right, respectively), but at intermediate concentrations (3–30 μ M) increases MBR in hiPSC-derived cocultures (Figure 3B, middle), whereas there is no change in the rat primary cortical culture.

Muscarinic acetylcholine receptor agonist. Pilocarpine increases MSR in hiPSC-derived neuronal cocultures following exposure to 1 μ M, but decreases MSR and MBR following exposure to 30 μ M (Figs. 4A and 4B). In rat primary cortical cultures, pilocarpine has little effect on MSR and MBR. Pilocarpine has little effect on MNBR of hiPSC-derived cocultures. In rat primary cortical cultures, pilocarpine strongly increases network bursting following exposure to 3 and 10 μ M, but not at 30 μ M (Figure 4C).

Potassium channel blocker. Linopirdine concentration-dependently decreases MSR in hiPSC-derived cocultures, in contrast to rat primary cortical cultures where a biologically relevant increase is observed (Figure 5A). MBR increases significantly following exposure to 3 μ M linopirdine in hiPSC-derived cocultures, followed by a decrease at higher test concentrations (Figure 5B). This trend is not observed in rat primary cortical cultures where MBR is not affected by linopirdine. At high concentrations (30–100 μ M), linopirdine decreases MNBR of hiPSC-derived cocultures (Figure 5C). In rat primary cortical cultures, linopirdine increases MNBR but only at high concentrations (10–100 μ M).

Inhibitory compounds. CPZ (0.1–3 μ M) increases MSR in hiPSC-derived cocultures followed by a decrease at the highest test concentration (10 μ M; Figure 6A, left). CPZ has little effect on MSR in rat primary cortical cultures, except for a decrease at the highest test concentration. A comparable trend is observed for

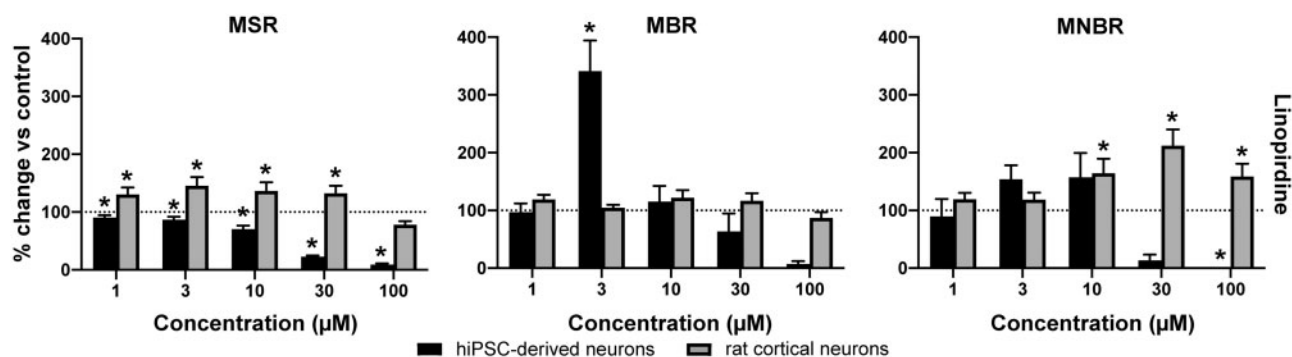


Figure 5. Effects of modulation of human-induced pluripotent stem cell (hiPSC)-derived cocultures (black) and rat primary cortical cultures (gray) with linopirdine on mean spike rate (A), mean burst rate (B), and mean network burst rate (C). Effects are depicted as average % change of control (solvent control set to 100%; dashed line) \pm SEM from $n = 7$ –12 wells for hiPSC-derived neuronal cocultures and $n = 26$ –29 wells for rat primary cortical cultures. * indicates a hit.

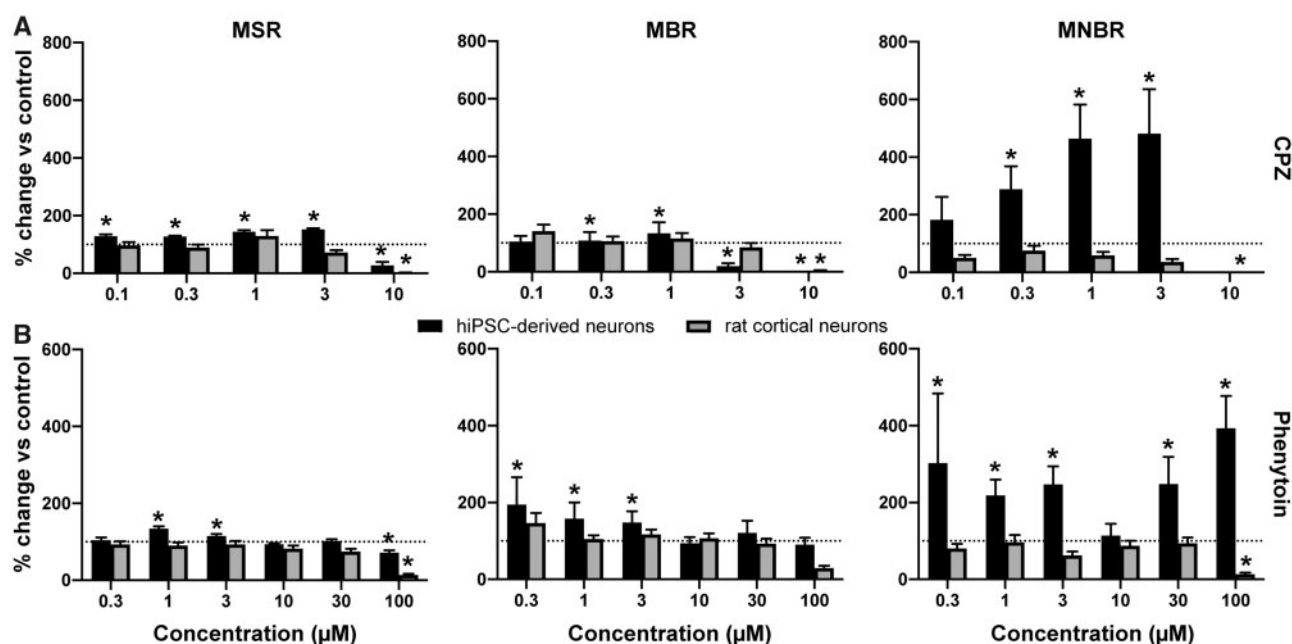


Figure 6. Effects of modulation of human-induced pluripotent stem cell (hiPSC)-derived cocultures (black) and rat primary cortical cultures (gray) with chlorpromazine (A) and phenytoin (B) on mean spike rate (left), mean burst rate (middle), and mean network burst rate (right). Effects are depicted as average % change of control (solvent control set to 100%; dashed line) \pm SEM from $n = 4$ –16 wells plates for hiPSC-derived neuronal cocultures and $n = 21$ –32 wells for rat primary cortical cultures. * indicates a hit.

MBR: in hiPSC-derived cocultures CPZ increases MBR, whereas MBR decreases at high concentrations. CPZ has little effect on MBR in rat primary cortical cultures, except for a decrease at the highest test concentration (Figure 6A, middle). At low concentrations, MNBR increases in hiPSC-derived cocultures following exposure to CPZ, which is followed by a decrease at the highest test concentration. CPZ has little effect on MNBR in rat primary cortical cultures, except for a decrease at the highest test concentration (Figure 6A, right).

Phenytoin decreases MSR in both models at the highest test concentration in a biologically relevant way (Figure 6B, left), although MSR is increased in hiPSC-derived cocultures at intermediate concentrations (1–3 μM). At low-test concentrations, MBR increases in hiPSC-derived cocultures, whereas MBR is not affected in rat primary cortical cultures (Figure 6B, middle). MNBR increases following phenytoin exposure in hiPSC-derived neuronal cocultures (Figure 6B, right). Phenytoin has little effect on MNBR in rat primary cortical cultures, except for a decrease at 100 μM.

Finger Prints of the Different Compound Classes

Heatmaps of the concentration-response curve of all tested compounds on hiPSC-derived neuronal cocultures and rodent primary cortical cultures were created to further illustrate the effect on different parameters. These heatmaps also visualize that compounds with the same mode of action have a comparable chemical fingerprint (Figs. 7–9). Because these heatmaps show more parameters than just the classical activity parameters as depicted in Figures 2–6, they create a more complete overview of how a network is affected by exposure. For example, when looking at the heatmaps, it is immediately clear that parameters such as (network) burst percentage, mean and median ISI within (network) burst and area under cross correlation are strongly affected by exposure to these (non)seizurogenic compounds. These heatmaps thus provide a valuable tool for visualizing changes in neuronal networks following modulation, including potential seizurogenicity patterns as described by Bradley et al. (2018).

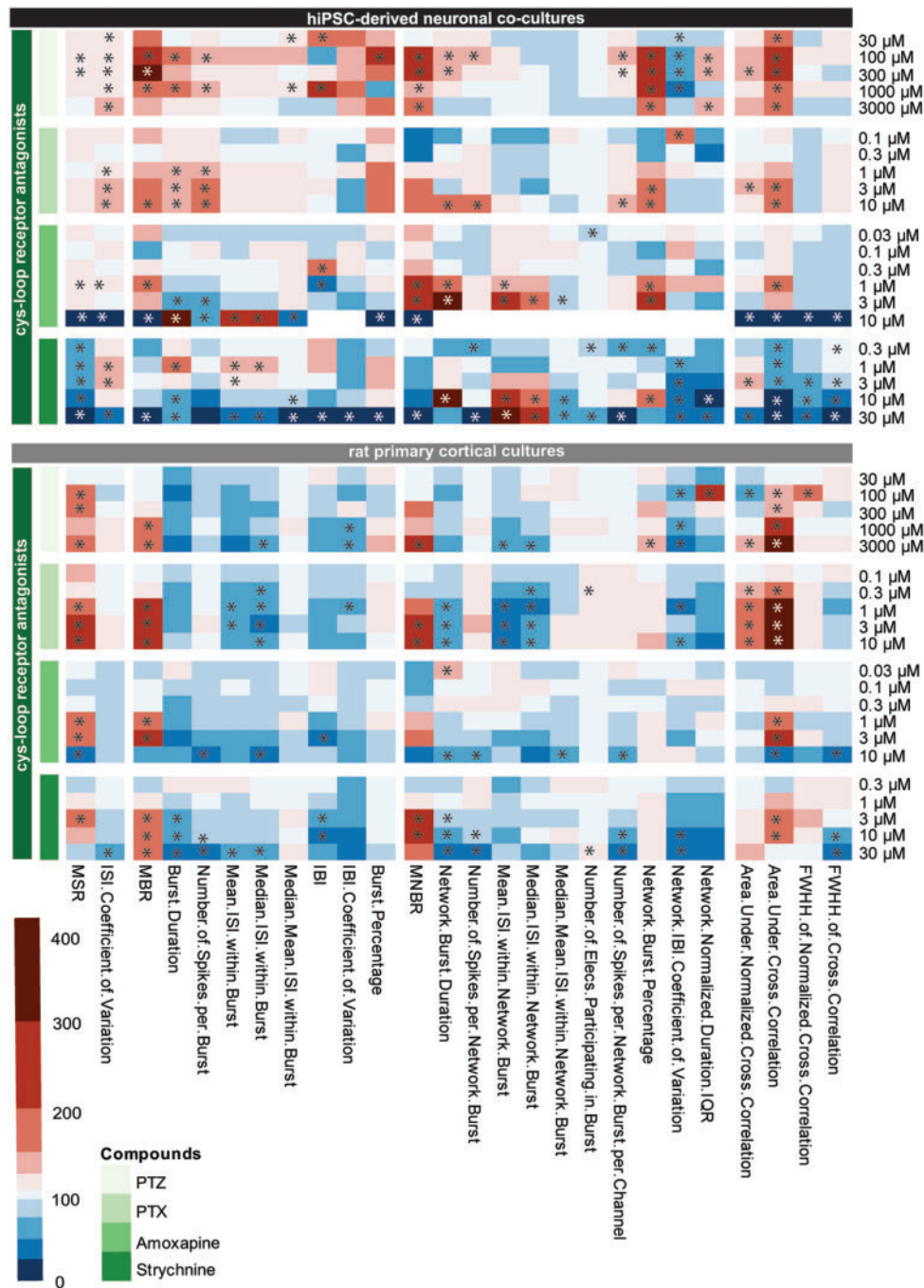


Figure 7. Heatmap of the effects of cys-loop antagonists (green, from top to bottom: pentylentetrazol, picrotoxin [PTX], amoxapine, and strychnine) on human-induced pluripotent stem cell (hiPSC)-derived neuronal cocultures (black, top) and rat primary cortical cultures (gray, bottom). Color scaling is based on the percentage of change relative to the control with red indicating an increase and blue a decrease. Asterisks indicate a hit. White areas indicate that no average could be calculated. Data are based on $n = 1\text{--}17$ wells for hiPSC-derived neuronal cocultures and $n = 9\text{--}32$ wells for rat primary cortical cultures. PTX and strychnine data have been published previously in Tukker et al. (2020).

When the hiPSC-derived neuronal cocultures are exposed to PTZ or PTX, both GABA_A-R antagonists, a comparable pattern occurs and strongest effects can be seen on burst-related parameters (Figure 7, left). However, effects are more profound following exposure to PTZ compared with PTX. Exposure of hiPSC-derived cocultures to amoxapine, also a GABA_A-R antagonist, increases MSR, MBR, MNBR, network burst duration, and the area under cross correlation, just like PTZ and PTX. However, the strong increasing effect on burst-related

parameters is not so clear following exposure to amoxapine. Following exposure to PTZ and amoxapine, the intermediate concentrations have the strongest effect on burst and network burst rate. The fourth compound in the cys-loop receptor antagonist category, strychnine, shows a different pattern with a clear decrease in activity in hiPSC-derived cocultures. This is also the only compound with a different target, the glycine receptor. Exposure of rat primary cortical cultures to the same set of cys-loop receptor antagonists yields a pattern different from

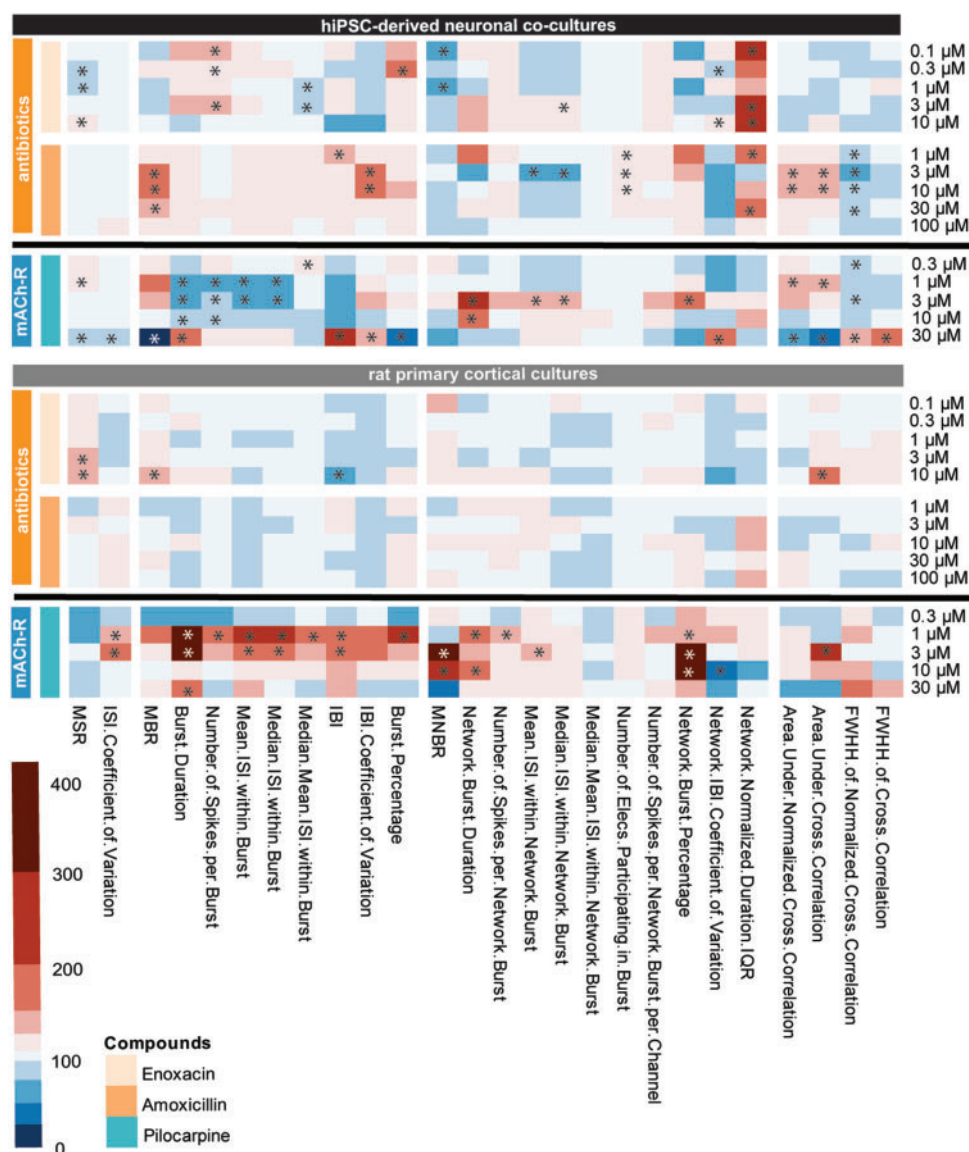


Figure 8. Heatmap of the effects of antibiotics (orange, from top to middle: enoxacin and amoxicillin) and a muscarinic acetylcholine receptor agonist (blue, bottom: pilocarpine) on human-induced pluripotent stem cell (hiPSC)-derived neuronal cocultures (black, top) and rat primary cortical cultures (gray, bottom). Color scaling is based on the percentage of change relative to the control with red indicating an increase and blue a decrease. Asterisks indicate a hit. Data are based on $n = 8$ –12 wells for hiPSC-derived neuronal cocultures and $n = 20$ –35 wells for rat primary cortical cultures.

the pattern of hiPSC-derived neuronal cocultures (Figure 7, right). Overall, activity decreases following exposure of rat primary cortical cultures. The pattern for all 4 compounds is comparable, with increases in MSR, MBR, MNBR, and the area under cross correlation.

The next group consists of 2 antibiotics, both GABA_A-receptor antagonists (Figure 8, orange: enoxacin and amoxicillin). When looking at the pattern resulting from exposure of hiPSC-derived cocultures it can be seen that the magnitude of change of effects is less than with the other GABA_A-receptor antagonists PTZ and PTX. Exposure of rat primary cortical cultures results in even milder effects (Figure 8, right). In the case of exposure to amoxicillin, no effects can be observed in rat primary cortical cultures.

Exposure of both models to the mACh receptor agonist pilocarpine (Figure 8, blue: bottom) results in a pattern that indicates this different mode of action as it has few similarities with other

compounds. For both hiPSC-derived neuronal cocultures and rat primary cortical cocultures it can be seen that exposure to the intermediate concentrations results in the biggest effect. Other than that, there are few similarities between the pattern in hiPSC-derived neuronal cocultures and rat primary cortical cocultures.

Two potassium channel blockers were tested (Figure 9, purple: linopirdine and 4-AP). For neither cell model it is clear from the heatmap that the compounds have the same mode of action. In both cell models, linopirdine affects network burst parameters strongest, whereas 4-AP has more effect on burst-related parameters.

The last group consists of 2 inhibitory compounds (Figure 9, pink: CPZ and phenytoin). CPZ has the D2-receptor as a target and strongly increases MBR, MNBR, and network burst percentage and decreases the IBI in hiPSC-derived neuronal networks. This same increase can be observed when hiPSCs are exposed to phenytoin, a sodium channel blocker. Both compounds have

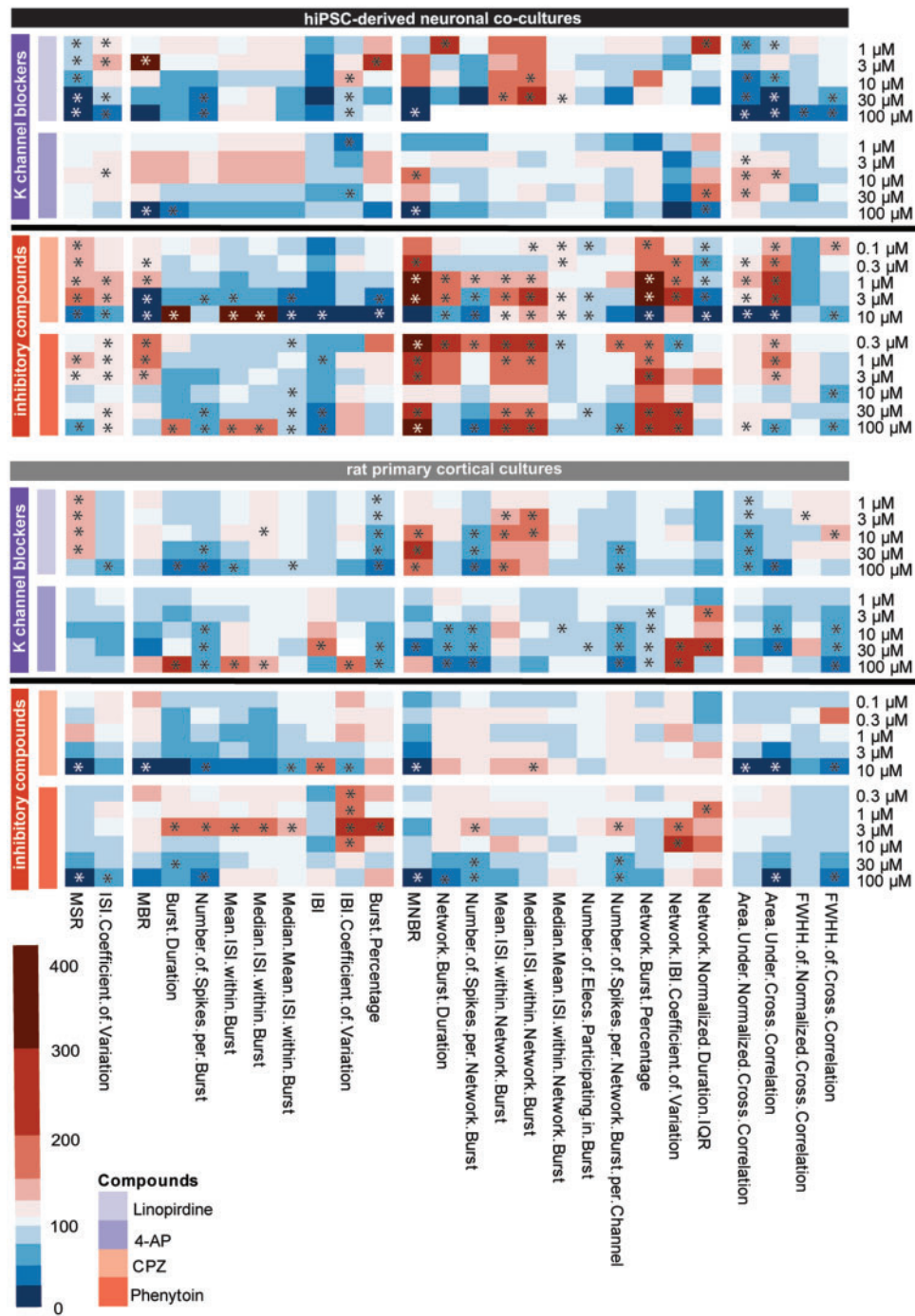


Figure 9. Heatmap of the effects of potassium channel blockers (purple, linopirdine and aminopyridine [4-AP]) and inhibitory compounds (red, chlorpromazine and phenytoin) on human-induced pluripotent stem cell (hiPSC)-derived neuronal cocultures (black, top) and rat primary cortical cultures (gray, bottom). Color scaling is based on the percentage of change relative to the control with red indicating an increase and blue a decrease. Asterisks indicate a hit. Data are based on $n = 1\text{--}16$ wells for hiPSC-derived neuronal cocultures and $n = 5\text{--}31$ wells for rat primary cortical cultures. 4-AP data have been published previously in [Tukker et al. \(2020\)](#).

relatively mild effects on spike parameters. When rat primary cortical cultures are exposed to CPZ or phenytoin, spike parameters decrease. Also, bursting and network bursting decrease with increasing concentration. Overall, effects on rat primary cortical cultures are milder than on hiPSC-derived cocultures.

PCA to Distinguish Between Human and Rodent Model

In order to visualize the potential interspecies differences following exposure to GABA_A receptor antagonists (PTZ, PTX,

amoxapine, enoxacin, and amoxicillin) between the hiPSC-derived neuronal coculture and rat primary cortical culture, a PCA was performed. PCA efficiently clusters MEA data based on the activity profile of the networks following exposure.

Parameters for the PCA were selected based on visual inspection of a correlation matrix ([Supplementary Table 12](#)) and the heatmaps ([Figs. 7–9](#)). A PCA was performed on 10 items (5 compounds per model) and 14 parameters. Four principal components have an eigenvalue > 1 . Together, these components

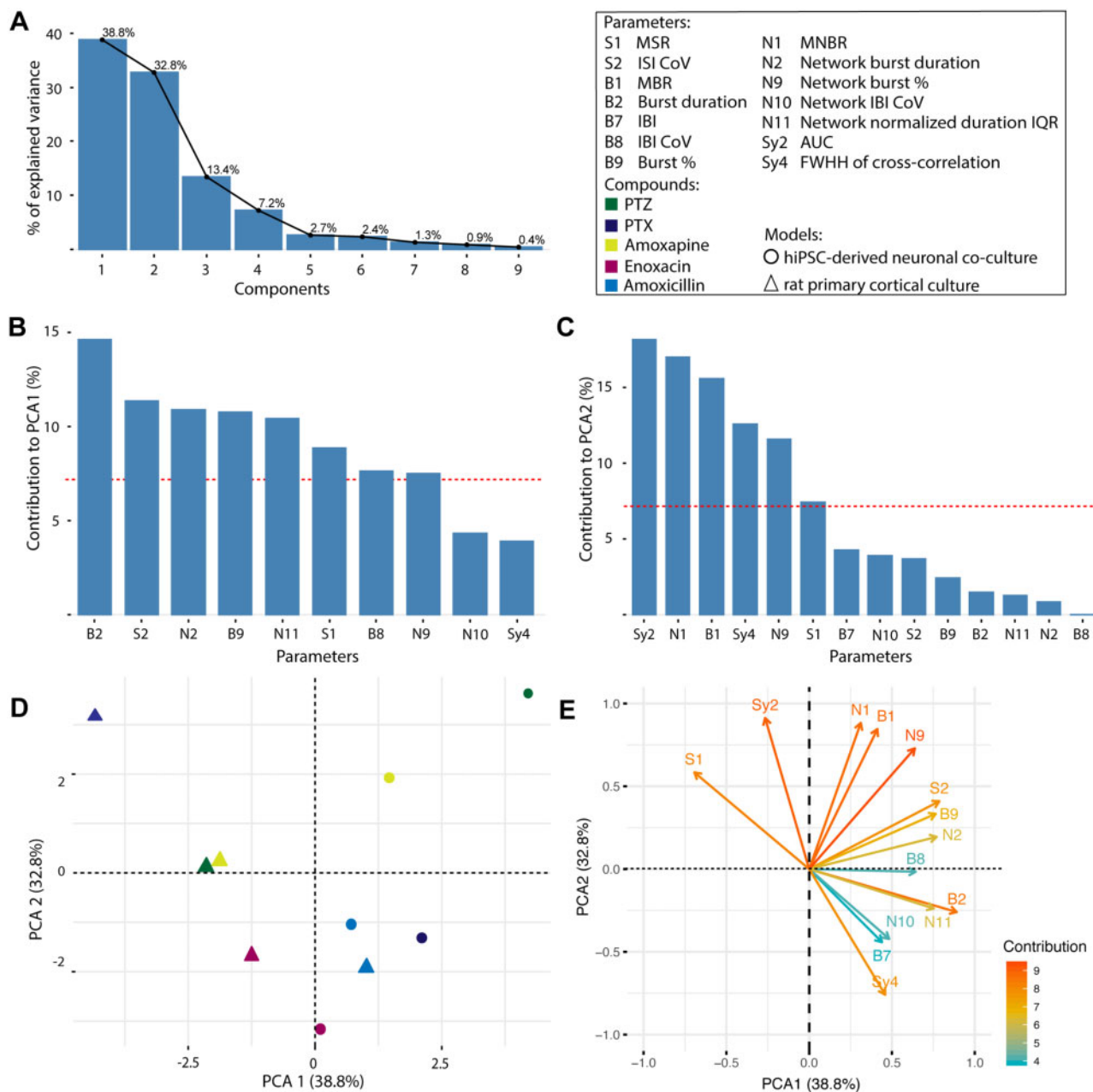


Figure 10. Scree plot displaying the percentage of variety explained by each component (A) for different GABA_A receptor antagonists. Contribution of each parameter to principal component analysis (PCA) 1 (B) and PCA2 (C). The red line indicates the expected contribution (7%). Bars above the red line indicate parameter importance for the component. The individual compounds are plotted in circles (human-induced pluripotent stem cell-derived neuronal coculture) and triangles (rat primary cortical cultures) visualizing a clear segregation between the 2 models (D). Plot depicting the contribution of parameters to the 2 components in arrows, darker orange arrows indicate higher contribution, whereas arrows in blue depict parameters with a lower contribution (E). Amount of variation explained by a principal component is indicated in parenthesis (D/E).

explain 92.2% of the variability as becomes clear from the scree plot (Figure 10A). In total, 8 parameters score higher than the expected 7% contribution to component 1 (Figure 10B) and 5 parameters for component 2 (Figure 10C). Notably, the most important parameters contributing to PCA1 relate to duration of (network) bursts and the percentage of spikes that occur in (network) bursts. This is in contrast to PCA2 where classical activity parameters (MBR and MNBR) as well as parameters related to synchronicity are more important. What becomes apparent from the plot (Figure 10D) is that there is a clear segregation between data points from hiPSC-derived neuronal cocultures and

rat primary cortical neurons. With the exception of amoxicillin, all rat primary cortical culture data are presented in left quadrants of the graph, whereas the hiPSC-derived neuronal coculture data are presented in the right quadrants. Contribution of the different parameters to the 2 components is depicted in Figure 10E. Interestingly, the MSR has a strong negative contribution to PCA1 (Figure 10E).

Comparison of Seizure Liability Between the 2 Models

In order to compare the suitability and sensitivity for seizure liability assessment between the 2 models, for all compounds

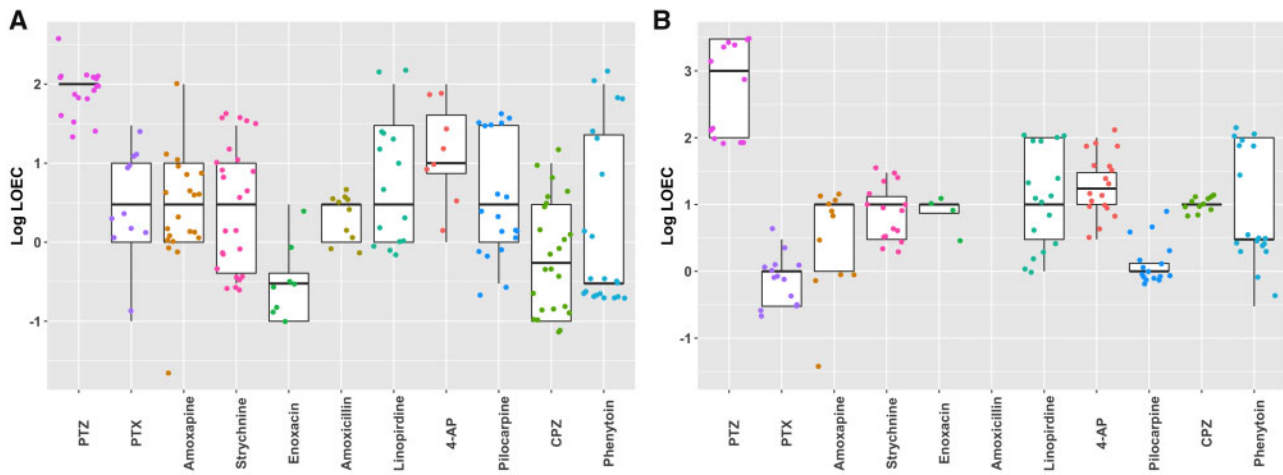


Figure 11. Boxplots depicting Lowest observed effect concentration (LOECs) of the different metric parameters per compound on human-induced pluripotent stem cell (hiPSC)-derived neuronal cocultures (A) and rat primary cortical cultures (B). No LOEC could be determined for amoxicillin on the rat primary cortical culture.

Table 3. Lowest LOECs of the 26 Parameters in μM for the Human and Rodent Cell Model

	hiPSC-Derived Neuronal Coculture	Rat Primary Cortical Culture
PTZ	30	100
PTX	0.1	0.3
Amoxapine	0.03	0.03
Strychnine	0.3	3
Enoxacin	0.1	3
Amoxicillin	1	–
Linopirdine	1	1
4-AP	1	3
Pilocarpine	0.3	0.3
CPZ	0.1	10
Phenytoin	0.3	3

LOECs in bold illustrate the lowest LOEC (ie, most sensitive) in case there is a difference between the 2 models. – indicates no LOEC could be calculated.

LOECs (defined as lowest hit concentration) were calculated for all 26 metric parameters (Figure 11). LOECs were compared between the 2 models. The model with the lowest LOEC is defined as the most sensitive model. For most tested compounds, the hiPSC-derived neuronal culture is more sensitive (Table 3). Sensitivity is equal between the 2 cultures for exposure to amoxapine, linopirdine and pilocarpine. No LOECs could be determined following exposure of rat primary cortical cultures to amoxicillin.

DISCUSSION

The aim of this study was to assess the suitability of hiPSC-derived neuronal cocultures for seizure liability assessment using MEA-recordings. We compared data obtained with human neuronal cocultures with data obtained in parallel from rat primary cortical cultures.

Our MEA recordings (Figs. 2–6) show that this type of experiment is suitable for the detection of changes in network activity following modulation by different drugs. Parameters that are important for *in vitro* seizure liability assessment include parameters that describe the activity and the organization of the activity (Bradley et al., 2018). Examples of these parameters

are spike, and (network) burst rate, but also the percentage of spikes that is incorporated in (network) bursts as well as parameters related to synchronicity. Importance of these parameters becomes clear from the heatmaps (Figs. 7–9) and PCA (Figure 10). If *in vitro* seizures are defined by changes in these aforementioned parameters, then our data confirm that both models despite the differences, are able to detect seizure liability *in vitro*. No changes were detected following exposure to amoxicillin in the rodent culture. However, sensitivity for the different test compounds differs between the human and rodent model as becomes clear when comparing LOECs (Figure 11 and Table 3). Our heatmaps indicate that it is possible to create fingerprint and group compounds with comparable mechanisms of action (Figs. 7 and 8). From these heatmaps, it becomes clear that burst and network burst parameters are more sensitive for excitatory changes in hiPSC-derived cocultures than in rat primary cortical cultures. Spike parameters are more affected in rodent primary cultures than in hiPSC-derived cocultures. Our PCA shows that it is possible to differentiate within a subset of compounds with a similar mode of action between 2 cell models (Figure 10).

Looking at just PTZ, a compound used to induce seizures in laboratory rodents (Klioueva et al., 2001; Singh et al., 2019) and thus a known seizurogenic compound, activity increased in both the rodent and hiPSC-derived neuronal network model at concentrations comparable with concentrations reported in literature (Figure 2A; Bradley et al., 2018; Kreir et al., 2018). The observed trend of increased bursting after PTZ exposure on hiPSC-derived cocultures, followed by a decrease at higher concentrations, is comparable with previous studies (Odawara et al., 2018). The cyclic antidepressant amoxapine is known to cause seizures as an adverse drug reaction (Kumlien and Lundberg, 2010; Litovitz and Troutman, 1983). Not surprisingly, amoxapine increased activity in both models (Figure 2B). Increase in network activity was only observed in the hiPSC-derived neuronal coculture. However, in both models, activity decreased to a minimum at the highest concentration tested. A previous study reported no significant change in spike rate following exposure of rat primary cortical cultures to amoxapine (Kreir et al., 2018), nor did this research find seizures *in vivo* when rats were dosed intravenously, indicating a potential interspecies difference in amoxapine sensitivity.

The fluoroquinolone antibiotic enoxacin is known to cause seizures as adverse drug reaction (Simpson and Brodie, 1985). Decreases in activity were found in the hiPSC-derived model following enoxacin exposure (Figure 3A), whereas in the rodent cell culture model, spike and burst rate did increase. However, in rat hippocampal slices, seizures were found at 30 μ M (Gao et al., 2017). This is above our highest test concentration. Exposure to the penicillin antibiotic amoxicillin had a more profound effect on hiPSC-derived cocultures as compared with rat primary cortical cultures (Figure 3B), with an increase in burst rate. Lack of effect on rat primary cortical cultures following amoxicillin exposure is in line with previous reports (McConnell et al., 2012). However, amoxicillin has been reported to cause seizures as an adverse drug reaction in humans (Raposo et al., 2016). This thus matches our hiPSC-derived neuronal data.

When looking at the GABA_A receptor antagonists (PTZ, PTX, amoxapine, enoxacin, and amoxicillin) as a group in the heatmap (Figs. 7 and 8), it can be observed that all increased the overall activity in both models, with the exception of enoxacin on the hiPSC-derived neuronal coculture. However, burst duration did not increase following exposure of rat primary cortical cultures. This is in contrast to hiPSC-derived cocultures, where an increase in burst duration was frequently observed. The hiPSC-derived cocultures thus follow pattern 1. Bradley et al. (2018) named amoxapine as a compound following pattern 2. However, that was based on an exposure of 5 μ M. Our data indicate that activity and network synchronicity decreased between 3 and 10 μ M on both models following amoxapine exposure. At this point, seizurogenic pattern 2 can be observed (Figure 7), indicating that at low-test concentrations amoxapine follows pattern 1 and then at higher concentrations pattern 2. Both antibiotics, enoxacin and amoxicillin, are GABA_A receptor antagonists and follow pattern 1 in both models. However, in both models and with both compounds, the observed effect is not as strong as with the other GABA_A receptor antagonists. Overall, the increased network organization and synchronicity are more pronounced following exposure of hiPSC-derived cocultures as compared with rat primary cortical cultures. The differences between the human and rodent model following exposure to GABA_A receptor antagonists were confirmed by PCA (Figure 10). This analysis efficiently identified differences between the 2 models and thus emphasizes interspecies differences. In this study, PCA has been performed on one set of compounds with a similar mode of action. However, this type of analysis holds great potential for further identifying differences and similarities between models following exposure to groups of compounds with other modes of action. Strychnine has been shown to follow pattern 2. In our data, exposure of hiPSC-derived cocultures to strychnine clearly results in pattern 2 (Figure 7). In the case of rodent primary cortical cultures activity increases. However, network organization decreases in line with pattern 2, as reflected in the decreased ISI CoV, burst duration and burst percentage.

Pilocarpine is used to model epilepsy *in vivo* in rodents (Marchi et al., 2007). At low-test concentrations pilocarpine increased activity of hiPSC-derived neuronal cocultures, but at the highest test concentration a decrease was observed (Figs. 3A and 3B). This biphasic effect with a strong decrease in activity following exposure to high concentrations has been reported for other compounds such as endosulfan, lindane, and fipronil (Dingemans et al., 2016; Wallace et al., 2015). It could also be the result of receptor desensitization or of a nonspecific effect on ion channels, such as inhibition of voltage-gated calcium channels (Heusinkveld et al., 2010). Rat primary cortical cultures

showed a strong increase in network burst activity, in line with other studies that reported seizurogenic effects on rodent primary cultures and hippocampal slices following exposure to comparable concentrations (Kreir et al., 2018; Nagao et al., 1996). The data presented here do not allow for a clear indication that pilocarpine follows either seizurogenic pattern. This problem was also mentioned by Bradley et al. (2018).

In both tested models, linopirdine decreased activity, except network burst activity in the rodent model (Figure 5) at concentrations in line with previous reports (Bradley et al., 2018). Exposure of rat primary cortical cultures to linopridine (60 μ M) has been shown to result in seizurogenic pattern 2 (Bradley et al., 2018). Our data showed that in both models exposure to linopirdine at a comparable concentration resembles pattern 2 (Figure 8). The other potassium channel blocker shown (Figure 8), 4-AP, should resemble pattern 1 (Bradley et al., 2018). However, this is not clear from our data.

CPZ increased spiking activity in hiPSC-derived neuronal cocultures (Figure 6A). At higher test concentrations activity decreased. Bursting and network bursting decreased following exposure to this compound. These findings are in line with literature (Kreir et al., 2018). In rat hippocampal slices, CPZ has been shown to induce seizures at 1–10 μ M (Easter et al., 2007), in line with our hiPSC-derived data. Exposure of hiPSC-derived cocultures to CPZ results in pattern 1. However, this pattern cannot be observed in rat primary cortical cultures.

Phenytoin is designed as an antiepileptic drug and therefore expected to decrease network activity. Phenytoin (Figure 6B) decreases activity at the highest test concentration in hiPSC-derived cocultures, at similar concentrations as others found with hiPSC-cultures (Odawara et al., 2018). Pattern 1 can be observed when hiPSC-derived cocultures are exposed to phenytoin, whereas this is not clear in rat primary cortical cultures (Figure 8).

There are several factors that could contribute to the observed differences between the 2 models. It must be kept in mind that the medium of the rodent cortical culture contains serum, whereas the medium of the hiPSC-derived cocultures is serum free. Therefore, the bioavailability of test compounds might be slightly lower in the rodent culture due to serum-compound interactions. Also, there is a difference between the 2 cultures in the percentage of astrocytes present. The rat primary cortical culture contains about 45% astrocytes (Görtz et al., 2004; Tukker et al., 2016). The percentage of astrocytes in the hiPSC-derived neuronal coculture can easily be increased. However, using higher percentages of astrocytes in the iPSC-derived cultures hampers spontaneous neuronal activity and (network) bursting, likely due to profound cell clustering. On the data analysis side, it is important to note that defining “hits” in this way may make the method less sensitive for decreases in activity. Therefore, a reduction in activity will less likely be a hit than an increase. However, this should not be a major issue for seizure liability assessment.

We have shown that hiPSC-derived cocultures can be used already as an initial screen for seizurogenic activity *in vitro*. Our data indicate differences between the human and rodent model, highlighting the need to move towards human iPSC-derived neuronal coculture models for more predictive *in vitro* seizure liability assessment. This need is emphasized by the fact that the hiPSC-derived model seems to be more sensitive than the primary rodent cortical culture model. However, these hiPSC-derived neuronal cells must be further characterized. Also, this approach must be thoroughly validated using a larger set of test compounds including compounds that are known to

cause seizures *in vivo* and negative controls before they can replace the current gold standard of rodent primary cortical cultures.

SUPPLEMENTARY DATA

Supplementary data are available at Toxicological Sciences online.

ACKNOWLEDGMENT

We gratefully acknowledge members of the Neurotoxicology Research Group for helpful discussions.

FUNDING

National Centre for the Replacement, Refinement and Reduction of Animals in Research (NC3Rs; project number 50308-372160); the Faculty of Veterinary Medicine (Utrecht University, The Netherlands).

DECLARATION OF CONFLICTING INTERESTS

The authors declared no potential conflicts of interest with respect to the research, authorship, and/or publication of this article.

REFERENCES

- Accardi, M. V., Huang, H., and Authier, S. (2018). Seizure liability assessments using the hippocampal tissue slice: Comparison of non-clinical species. *J. Pharmacol. Toxicol. Methods* **93**, 59–68.
- Alachkar, A., Łażewska, D., Latacz, G., Frank, A., Siwek, A., Lubelska, A., Honkisz-Orzechowska, E., Handzlik, J., Stark, H., Kieć-Kononowicz, K., et al. (2018). Studies on anticonvulsant effects of novel histamine h3r antagonists in electrically and chemically induced seizures in rats. *Int. J. Mol. Sci.* **19**, 3386. Available at: <http://www.mdpi.com/1422-0067/19/11/3386>. Accessed September 17, 2019.
- Aminoshariae, A., and Khan, A. (2015). Acetaminophen: old Drug, New Issues. *J Endod* **41**, 588–593. Available at: <http://dx.doi.org/10.1016/j.joen.2015.01.024>. Accessed December 20, 2018.
- Anson, B. D., Kolaja, K. L., and Kamp, T. J. (2011). Opportunities for use of human iPS cells in predictive toxicology. *Clin. Pharmacol. Ther.* **89**, 754–758.
- Arrowsmith, J., and Miller, P. (2013). Phase II and Phase III attrition rates 2011–2012. *Nat. Rev. Drug Discov.* **12**, 569–569. Available at: <http://www.nature.com/articles/nrd4090>. Accessed September 4, 2019.
- Authier, S., Arezzo, J., Delatte, M. S., Kallman, M.-J., Markgraf, C., Paquette, D., Pugsley, M. K., Ratcliffe, S., Redfern, W. S., Stevens, J., et al. (2016). Safety pharmacology investigations on the nervous system: An industry survey. *J. Pharmacol. Toxicol. Methods* **81**, 37–46. Available at: <https://www.science-direct.com/science/article/pii/S1056871916300570> via %3Dihub. Accessed January 16, 2019.
- Boyd-Kimball, D., Gonczy, K., Lewis, B., Mason, T., Siliko, N., and Wolfe, J. (2018). Classics in chemical neuroscience: Chlorpromazine. *ACS Chem. Neurosci.* Available at: <http://pubs.acs.org/doi/10.1021/acschemneuro.8b00258>. Accessed December 20, 2018.
- Bradley, J. A., Luithardt, H. H., Metea, M. R., and Strock, C. J. (2018). In vitro screening for seizure liability using microelectrode array technology. *Toxicol. Sci.* **163**, 240–253. Available at: <https://academic.oup.com/toxsci/article/163/1/240/4844105>. Accessed August 28, 2018.
- Burn, D. J., Tomson, C. R. V., Seviour, J., and Dale, G. (1989). Strychnine poisoning as an unusual cause of convulsions. *Postgrad. Med. J.* **65**, 563–564.
- Buskila, Y., Breen, P. P., Tapson, J., van Schaik, A., Barton, M., and Morley, J. W. (2015). Extending the viability of acute brain slices. *Sci. Rep.* **4**, 5309. Available at: <http://www.ncbi.nlm.nih.gov/pubmed/24930889>. Accessed May 6, 2019.
- Cook, D., Brown, D., Alexander, R., March, R., Morgan, P., Satterthwaite, G., and Pangalos, M. N. (2014). Lessons learned from the fate of AstraZeneca's drug pipeline: A five-dimensional framework. *Nat. Rev. Drug Discov.* **13**, 419–431.
- Cotterill, E., Charlesworth, P., Thomas, C. W., Paulsen, O., and Eglen, S. J. (2016). A comparison of computational methods for detecting bursts in neuronal spike trains and their application to human stem cell-derived neuronal networks. *J. Neurophysiol.* **116**, 306–321. Available at: <http://www.ncbi.nlm.nih.gov/pubmed/27098024>. Accessed December 20, 2018.
- De Sarro, A., Zappalá, M., Chimirri, A., Grasso, S., and De Sarro, G. B. (1993). Quinolones potentiate cefazolin-induced seizures in DBA/2 mice. *Antimicrob. Agents Chemother.* **37**, 1497–1503. Available at: <http://www.ncbi.nlm.nih.gov/pubmed/8395790>. Accessed December 20, 2018.
- Dhir, A. (2012). Pentylentetrazol (PTZ) kindling model of epilepsy. In: *Current Protocols in Neuroscience*, Vol. Chapter 9. John Wiley & Sons, Inc., Hoboken, NJ, pp. Unit 9.37. Available at: <http://www.ncbi.nlm.nih.gov/pubmed/23042503>. Accessed December 20, 2018.
- Dingemans, M. M. L., Schütte, M. G., Wiersma, D. M. M., de Groot, A., van Kleef, R. G. D. M., Wijnolts, F. M. J., and Westerink, R. H. S. (2016). Chronic 14-day exposure to insecticides or methylmercury modulates neuronal activity in primary rat cortical cultures. *Neurotoxicology* **57**, 194–202.
- Easter, A., Bell, M. E., Damewood, J. R., Redfern, W. S., Valentin, J.-P., Winter, M. J., Fonck, C., and Bialecki, R. A. (2009). Approaches to seizure risk assessment in preclinical drug discovery. *Drug Discov. Today* **14**, 876–884. Available at: <https://linkinghub.elsevier.com/retrieve/pii/S1359644609001895>. Accessed April 28, 2019.
- Easter, A., Sharp, T. H., Valentin, J. P., and Pollard, C. E. (2007). Pharmacological validation of a semi-automated *in vitro* hippocampal brain slice assay for assessment of seizure liability. *J. Pharmacol. Toxicol. Methods* **56**, 223–233.
- Fan, J., Thalody, G., Kwagh, J., Burnett, E., Shi, H., Lewen, G., Chen, S.-J., and Levesque, P. (2019). Assessing seizure liability using multi-electrode arrays (MEA). *Toxicol. In Vitro* **55**, 93–100. Available at: <https://linkinghub.elsevier.com/retrieve/pii/S0887233318303631>. Accessed May 6, 2019.
- Gao, M., Igata, H., Takeuchi, A., Sato, K., and Ikegaya, Y. (2017). Machine learning-based prediction of adverse drug effects: An example of seizure-inducing compounds. *J. Pharmacol. Sci.* **133**, 70–78.
- Gao, Z., Chen, Y., Cai, X., and Xu, R. (2016). Predict drug permeability to blood–brain-barrier from clinical phenotypes: Drug side effects and drug indications. *Bioinformatics* **33**, btw713. Available at: <https://academic.oup.com/bioinformatics/article-lookup/doi/10.1093/bioinformatics/btw713>. Accessed September 5, 2019.

- Görtz, P., Fleischer, W., Rosenbaum, C., Otto, F., and Siebler, M. (2004). Neuronal network properties of human teratocarcinoma cell line-derived neurons. *Brain Res.* **1018**, 18–25.
- Grainger, A. I., King, M. C., Nagel, D. A., Parri, H. R., Coleman, M. D., and Hill, E. J. (2018). In vitro models for seizure-liability testing using induced pluripotent stem cells. *Front. Neurosci.* **12**, 590. Available at: <https://www.frontiersin.org/article/10.3389/fnins.2018.00590/full>. Accessed May 6, 2019.
- Heusinkveld, H. J., Thomas, G. O., Lamot, I., van den Berg, M., Kroese, A. B. A., and Westerink, R. H. S. (2010). Dual actions of lindane (γ -hexachlorocyclohexane) on calcium homeostasis and exocytosis in rat PC12 cells. *Toxicol. Appl. Pharmacol.* **248**, 12–19. Available at: <http://www.ncbi.nlm.nih.gov/pubmed/20600211>. Accessed September 11, 2018.
- Hogberg, H. T., Sobanski, T., Novellino, A., Whelan, M., Weiss, D. G., and Bal-Price, A. K. (2011). Application of micro-electrode arrays (MEAs) as an emerging technology for developmental neurotoxicity: Evaluation of domoic acid-induced effects in primary cultures of rat cortical neurons. *Neurotoxicology* **32**, 158–168.
- Hondebrink, L., Verboven, A. H. A., Drega, W. S., Schmeink, S., De Groot, M., Van Kleef, R. G. D. M., Wijnolts, F. M. J., De Groot, A., Meulenbelt, J., and Westerink, R. H. S. (2016). Neurotoxicity screening of (illicit) drugs using novel methods for analysis of microelectrode array (MEA) recordings. *Neurotoxicology* **55**, 1–9.
- Izhikevich, E. M., Desai, N. S., Walcott, E. C., and Hoppensteadt, F. C. (2003). Bursts as a unit of neural information: Selective communication via resonance. *Trends Neurosci.* **26**, 161–167. Available at: <https://www.sciencedirect.com/science/article/pii/S0166223603000341>. Accessed December 21, 2018.
- Jiruska, P., de Curtis, M., Jefferys, J. G. R., Schevon, C. A., Schiff, S. J., and Schindler, K. (2013). Synchronization and desynchronization in epilepsy: Controversies and hypotheses. *J. Physiol.* **591**, 787–797. Available at: <http://www.ncbi.nlm.nih.gov/pubmed/23184516>. Accessed April 28, 2019.
- Johnstone, A. F. M., Gross, G. W., Weiss, D. G., Schroeder, O. H.-U., Gramowski, A., and Shafer, T. J. (2010). Microelectrode arrays: A physiologically based neurotoxicity testing platform for the 21st century. *Neurotoxicology* **31**, 331–350. Available at: <http://www.ncbi.nlm.nih.gov/pubmed/20399226>. Accessed September 5, 2019.
- Kapur, S., Cho, R., Jones, C., McKay, G., and Zipursky, R. B. (1999). Is amoxapine an atypical antipsychotic? Positron-emission tomography investigation of its dopamine₂ and serotonin₂ occupancy. *Biol. Psychiatry* **45**, 1217–1220. Available at: <https://www.sciencedirect.com/science/article/pii/S0006322398002042?via%3Dihub>. Accessed December 20, 2018.
- Kassambara, A., and Mundt, F. (2017). *Factoextra: Extract and visualize the results of multivariate data analyses*. R package version 1.0.5.
- Kawakami, J., Yamamoto, K., Asanuma, A., Yanagisawa, K., Sawada, Y., and Iga, T. (1997). Inhibitory effect of new quinolones on GABA_A receptor-mediated response and its potentiation with felbinac in xenopus oocytes injected with mouse-brain mRNA: Correlation with convulsive potency in vivo. *Toxicol. Appl. Pharmacol.* **145**, 246–254. Available at: <https://www.sciencedirect.com/science/article/pii/S0041008X97981370?via%3Dihub>. Accessed December 20, 2018.
- Klioueva, I. A., Van Luijckelaar, E. L. J. M., Chepurnova, N. E., and Chepurinov, S. A. (2001). PTZ-induced seizures in rats: Effects of age and strain. *Physiol. Behav.* **72**, 421–426.
- Kolde, R. (2019). *Pheatmap: Pretty heatmaps*. R package version 1.0.12.
- Kreir, M., Van Deuren, B., Versweyveld, S., De Bondt, A., Van den Wyngaert, I., Van der Linde, H., Lu, H. R., Teuns, G., and Gallacher, D. J. (2018). Do in vitro assays in rat primary neurons predict drug-induced seizure liability in humans? *Toxicol. Appl. Pharmacol.* **346**, 45–57. Available at: <https://www.sciencedirect.com/science/article/pii/S0041008X18301145>. Accessed June 20, 2019.
- Kuijlaars, J., Oyelami, T., Diels, A., Rohrbacher, J., Versweyveld, S., Meneghello, G., Tuefferd, M., Verstraelen, P., Detrez, J. R., Verschuuren, M., et al. (2016). Sustained synchronized neuronal network activity in a human astrocyte co-culture system. *Sci. Rep.* **6**, 36529.
- Kumlien, E., and Lundberg, P. O. (2010). Seizure risk associated with neuroactive drugs: Data from the WHO adverse drug reactions database. *Seizure* **19**, 69–73. Available at: <https://www.sciencedirect.com/science/article/pii/S1059131109002337?via%3Dihub>. Accessed December 20, 2018.
- Lê, S., Josse, J., and Husson, F. (2008). FactoMineR: An R Package for multivariate analysis. *J. Stat. Soft.* **25**, 1–18.
- Legéndy, C. R., and Salzman, M. (1985). Bursts and recurrences of bursts in the spike trains of spontaneously active striate cortex neurons. *J. Neurophysiol.* **53**, 926–939.
- Litovitz, T. L., and Troutman, W. G. (1983). Amoxapine overdose. Seizures and fatalities. *JAMA* **250**, 1069–1071. Available at: <http://www.ncbi.nlm.nih.gov/pubmed/6876345>. Accessed November 14, 2019.
- Little, D., Ketteler, R., Gissen, P., and Devine, M. J. (2019). Using stem cell-derived neurons in drug screening for neurological diseases. *Neurobiol. Aging* **78**, 130–141. Available at: <https://www.sciencedirect.com/science/article/pii/S0197458019300557>. Accessed April 12, 2019.
- Mackenzie, L., Medvedev, A., Hiscock, J. J., Pope, K. J., and Willoughby, J. O. (2002). Picrotoxin-induced generalised convulsive seizure in rat: Changes in regional distribution and frequency of the power of electroencephalogram rhythms. *Clin. Neurophysiol.* **113**, 586–596. Available at: <https://www.sciencedirect.com/science/article/pii/S1388245702000408>. Accessed September 17, 2019.
- Magalhães, D. M., Pereira, N., Rombo, D. M., Beltrão-Cavacas, C., Sebastião, A. M., and Valente, C. A. (2018). Ex vivo model of epilepsy in organotypic slices—a new tool for drug screening. *J. Neuroinflammation* **15**, 203. Available at: <https://jneuroinflammation.biomedcentral.com/articles/10.1186/s12974-018-1225-2>. Accessed March 23, 2020.
- Marchi, N., Oby, E., Batra, A., Uva, L., De Curtis, M., Hernandez, N., Van Boxel-Dezaire, A., Najm, I., and Janigro, D. (2007). In vivo and in vitro effects of pilocarpine: Relevance to ictogenesis. *Epilepsia* **48**, 1934–1946. Available at: <http://www.ncbi.nlm.nih.gov/pubmed/17645533>. Accessed December 20, 2018.
- Maslarova, A., Salar, S., Lapilover, E., Friedman, A., Veh, R. W., and Heinemann, U. (2013). Increased susceptibility to acetylcholine in the entorhinal cortex of pilocarpine-treated rats involves alterations in KCNQ channels. *Neurobiol. Dis.* **56**, 14–24. Available at: <https://www.sciencedirect.com/science/article/pii/S0969996113001095?via%3Dihub>. Accessed December 20, 2018.
- McConnell, E. R., McClain, M. A., Ross, J., LeFevre, W. R., and Shafer, T. J. (2012). Evaluation of multi-well microelectrode arrays for neurotoxicity screening using a chemical training set. *Neurotoxicology* **33**, 1048–1057.
- Meneghello, G., Verheyen, A., Van Ingen, M., Kuijlaars, J., Tuefferd, M., Van Den Wyngaert, I., and Nuydens, R. (2015). Evaluation of established human iPSC-derived neurons to

- model neurodegenerative diseases. *Neuroscience* **301**, 204–212.
- Nagao, T., Alonso, A., and Avoli, M. (1996). Epileptiform activity induced by pilocarpine in the rat hippocampal-entorhinal slice preparation. *Neuroscience* **72**, 399–408. Available at: <http://www.ncbi.nlm.nih.gov/pubmed/8737410>. Accessed November 14, 2018.
- Nicolas, J., Hendriksen, P. J. M., van Kleef, R. G. D. M., de Groot, A., Bovee, T. F. H., Rietjens, I. M. C. M., and Westerink, R. H. S. (2014). Detection of marine neurotoxins in food safety testing using a multielectrode array. *Mol. Nutr. Food Res.* **58**, 2369–2378.
- Odawara, A., Katoh, H., Matsuda, N., and Suzuki, I. (2016). Physiological maturation and drug responses of human induced pluripotent stem cell-derived cortical neuronal networks in long-term culture. *Sci. Rep.* **6**, 26181.
- Odawara, A., Matsuda, N., Ishibashi, Y., Yokoi, R., and Suzuki, I. (2018). Toxicological evaluation of convulsant and anticonvulsant drugs in human induced pluripotent stem cell-derived cortical neuronal networks using an MEA system. *Sci. Rep.* **8**, 10416. Available at: <http://www.ncbi.nlm.nih.gov/pubmed/29991696>. Accessed August 28, 2018.
- Onakpoya, I. J., Heneghan, C. J., and Aronson, J. K. (2016). Post-marketing withdrawal of 462 medicinal products because of adverse drug reactions: A systematic review of the world literature. *BMC Med.* **14**, 10. Available at: <https://bmcmmedicine.biomedcentral.com/articles/10.1186/s12916-016-0553-2>. Accessed April 28, 2019.
- Paavilainen, T., Pelkonen, A., Mäkinen, M. E.-L., Peltola, M., Huhtala, H., Fayuk, D., and Narkilahti, S. (2018). Effect of prolonged differentiation on functional maturation of human pluripotent stem cell-derived neuronal cultures. *Stem Cell Res.* **27**, 151–161.
- Peña, F., and Tapia, R. (2000). Seizures and neurodegeneration induced by 4-aminopyridine in rat hippocampus in vivo: Role of glutamate- and GABA-mediated neurotransmission and of ion channels. *Neuroscience* **101**, 547–561. Available at: <https://www.sciencedirect.com/science/article/pii/S0306452200004000>. Accessed September 17, 2019.
- Qiu, C., Johnson, B. N., and Tallent, M. K. (2007). K^+ M-current regulates the transition to seizures in immature and adult hippocampus. *Epilepsia* **48**, 2047–2058. Available at: <http://www.ncbi.nlm.nih.gov/pubmed/17651418>. Accessed December 20, 2018.
- Raposo, J., Teotónio, R., Bento, C., and Sales, F. (2016). Amoxicillin, a potential epileptogenic drug. *Epileptic Disord.* **18**, 454–457. Available at: <http://www.ncbi.nlm.nih.gov/pubmed/27900944>. Accessed December 21, 2018.
- Rogawski, M. A., and Löscher, W. (2004). The neurobiology of antiepileptic drugs. *Nat Rev Neurosci* **5**, 553–564. Available at: <http://www.nature.com/articles/nrn1430>. Accessed December 20, 2018.
- Sasaki, T., Suzuki, I., Yokoi, R., Sato, K., and Ikegaya, Y. (2019). Synchronous spike patterns in differently mixed cultures of human iPSC-derived glutamatergic and GABAergic neurons. *Biochem. Biophys. Res. Commun.* **513**, 300–305. Available at: <https://www.sciencedirect.com/science/article/pii/S0006291X19305613>. Accessed April 12, 2019.
- Simpson, K. J., and Brodie, M. J. (1985). Convulsions related to enoxacin. *Lancet* **326**, 161.
- Singh, N., Saha, L., Kumari, P., Singh, J., Bhatia, A., Banerjee, D., and Chakrabarti, A. (2019). Effect of dimethyl fumarate on neuroinflammation and apoptosis in pentylenetetrazol kindling model in rats. *Brain Res. Bull.* **144**, 233–245. Available at: <http://www.ncbi.nlm.nih.gov/pubmed/30472152>. Accessed December 20, 2018.
- Tukker, A. M., De Groot, M., Wijnolts, F. M. J., Kasteel, E. E. J., Hondebrink, L., and Westerink, R. H. S. (2016). Is the time right for in vitro neurotoxicity testing using human iPSC-derived neurons? *ALTEX* **33**, 261–271.
- Tukker, A. M., Van Kleef, R. G. D. M., Wijnolts, F. M. J., De Groot, A., and Westerink, R. H. S. (2020). Towards animal-free neurotoxicity screening: Applicability of hiPSC-derived neuronal models for in vitro seizure liability assessment. *ALTEX* **37**(1):121–135.
- Tukker, A. M., Wijnolts, F. M. J., De Groot, A., Wubbolts, R. W., and Westerink, R. H. S. (2019). *In Vitro Techniques for Assessing Neurotoxicity Using Human iPSC-Derived Neuronal Models*. Humana, New York, NY, pp. 17–35. Available at: http://link.springer.com/10.1007/978-1-4939-9228-7_2. Accessed May 25, 2019.
- Wallace, K., Strickland, J. D., Valdivia, P., Mundy, W. R., and Shafer, T. J. (2015). A multiplexed assay for determination of neurotoxicant effects on spontaneous network activity and viability from microelectrode arrays. *Neurotoxicology* **49**, 79–85.
- Zimmerman, T. J. (1981). 4. Pilocarpine. *Ophthalmology* **88**, 85–88. Available at: <https://www.sciencedirect.com/science/article/pii/S0161642081350726?via%3Dihub>. Accessed December 20, 2018.
- Zwartsen, A., Hondebrink, L., and Westerink, R. H. (2019). Changes in neuronal activity in rat primary cortical cultures induced by illicit drugs and new psychoactive substances (NPS) following prolonged exposure and washout to mimic human exposure scenarios. *Neurotoxicology* **74**, 28–39. Available at: <https://www.sciencedirect.com/science/article/pii/S0161813X18304352>. Accessed September 17, 2019.